Chain Conformation of Spacer Methylene Sequences for a Liquid Crystalline Polyether As Revealed by Solid-State ^{13}C NMR Spectroscopy

Hiroyuki Ishida and Fumitaka Horii*

Institute for Chemical Research, Kyoto University, Uji, Kyoto 611-0011, Japan

Received June 28, 2001

ABSTRACT: Solid-state ^{13}C NMR analyses of the structure and chain conformation have been carried out mainly at room temperature for a main-chain thermotropic liquid crystalline polyether which was newly polymerized from 3,3′-dimethyl-4,4′-dihydroxybiphenyl and 1,10-dibromodecane by using a phase transfer catalyst. This sample was crystallized by cooling from the melt through the nematic liquid crystalline state. Differential scanning calorimetry measurements and polarizing optical microscopic observations have confirmed that the nematic liquid crystalline phase appears in both heating and cooling processes. ^{13}C spin−lattice relaxation analyses have revealed that there exist three components with different T_{1C} values, which correspond to the crystalline, medium, and noncrystalline (supercooled liquid crystalline) components. By employing the difference in T_{1C}, the spectrum of each component is separately recorded, and the conformation of the CH_2 sequence is evaluated by considering the *γ-gauche* effect on the ^{13}C chemical shifts. As a result, the crystalline component is found to adopt the alternate *trans* (*t*) and *trans*−*gauche* exchange (*x*) conformation (*txtxtxtxt*), in good accord with the result separately obtained by the molecular dynamics simulation. In contrast, all the C−C bonds of the CH_2 sequence for the noncrystalline component are in the rapid *trans*−*gauche* exchange conformation (*xxxxxxxxx*), reflecting the same conformation in the liquid crystalline phase or at the melt.

Introduction

Main-chain thermotropic liquid crystalline polymers have been one of the focuses of increasing scientific and industrial interests during these past two decades due to their excellent mechanical, optical, and thermal properties.[1] However, the morphological structure as well as molecular level structure associated with the chain conformation and intermolecular interaction have not been well understood in relation to the molecular orientation and molecular motion in the liquid crystalline phase through which most materials are produced. In particular, time-dependent changes in molecular orientation and chain folding in the liquid crystalline phase before crystallization are almost unknown even at a qualitative level because of the lack of model liquid crystalline polymers suitable for such investigations. We have recently started a series of investigations associated with these basically important problems in the field of liquid crystalline polymer materials.

In a previous paper[2] we first reported the solid-state ^{13}C NMR analysis of the crystalline−noncrystalline structure and chain conformation performed at room temperature for main-chain thermotropic liquid crystalline polyurethane (UDMB-10, Scheme 1) which was composed of 3,3′-dimethyl-4,4′-biphenyldiyl units as mesogen and 10-CH_2 sequences as spacer. This sample, which was crystallized by cooling from the melt through the nematic liquid crystalline phase, was found to contain three components with different molecular mobilities assigned to the crystalline, medium, and noncrystalline (i.e., supercooled liquid crystalline) components. Moreover, it was clarified that the spacer CH_2 sequences adopt the characteristic conformation (*ttxtxtxtxtt*) composed of the *trans* (*t*) and *trans*−*gauche* exchange (*x*) conformations for the noncrystalline component whereas both crystalline and medium components simply take the planar zigzag conformation. In the case of another type of liquid crystalline polyether (HMS-9) similarly crystallized,[3] however, the most mobile component corresponding to the noncrystalline component was found to adopt the *xxxxxxxxx* conformation for the spacer CH_2 sequences like the case at the melt or in the nematic liquid crystalline phase. In contrast, the CH_2 sequences for the least mobile component, which is assignable to the crystalline component, were alternatively composed of the *xxtxxtxx* conformations.

Scheme 1

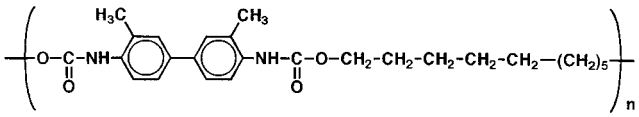

UDMB-10

Such great differences in spacer conformation for the two liquid crystalline polymers may be mainly due to the difference in chemical structures for the connecting parts between the mesogen units and the spacer CH_2 sequence, particularly to the presence or absence of the intermolecular hydrogen bonding associated with the urethane bonds. However, HMS-9 is composed of 4,4′-dihydroxy-α-methylstilbene residues and 9-CH_2 sequences, which are greatly different from the structures of the mesogen and spacer units for UDMB-10. In this paper, therefore, a new type of liquid crystalline polyether with the same mesogen and spacer units as for UDMB-10 are synthesized, and the spacer conformation is characterized in detail in each component included in this sample by the similar solid-state ^{13}C NMR analysis previously developed.[2,3] The difference in phase transition behavior between EDMB-10 and UDMB-10 will be also published somewhere, focusing on the effects of the cooling rate and molecular weight.

Experimental Section

Materials. *o*-Tolidine (from Tokyo Chemical Industry Co., Ltd.), 1,10-dibromodecane tetra-*n*-buthylammonium hydrogen

10.1021/ma011113l CCC: $20.00
Published on Web 09/28/2001

Scheme 2

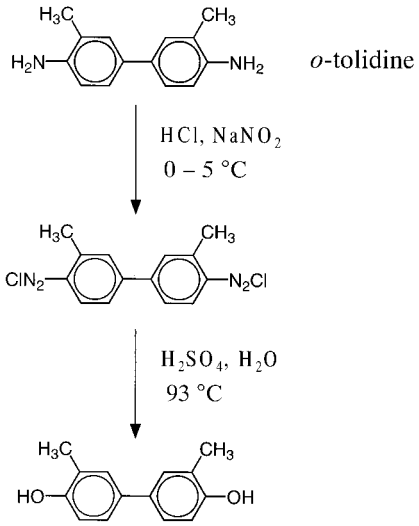

3,3'-dimethyl-4,4'-dihydroxybiphenyl (DMHB)

Scheme 3

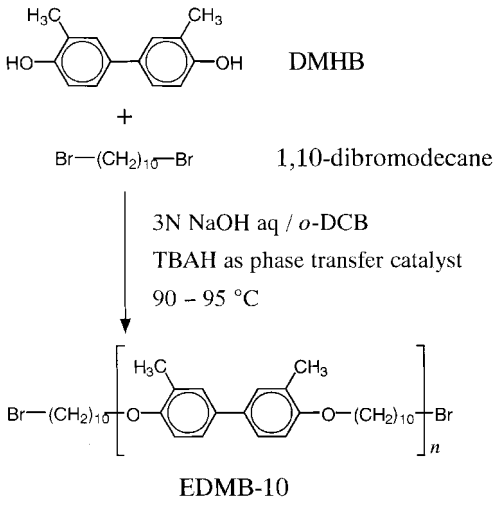

EDMB-10

o-DCB : *o*-dichlorobenzene

TBAH : tetra-*n*-buthylammonium hydrogen sulfate

sulfate (TBAH), and all other reagents (all from Nacalai Tesque Inc.) were used without further purification.

Synthesis of 3,3′-Dimethyl-4,4′-dihydroxybiphenyl (DMHB). Scheme 2 outlines the synthesis of DMHB on the basis of previous reports.[4−6] 4.24 g (20 mmol) of *o*-tolidine was made into a thin paste with 40 mL of water in a 200 mL beaker and a solution of 8.2 mL of concentrated hydrochloric acid in 20 mL of water was added slowly. After cooling below 5 °C with ice, a solution of 3.36 g (44 mmol) of sodium nitrite in 10 mL of water was further added from a dropping funnel. The resulting solution was stirred for 1.5 h, and then a diazonium solution was obtained. In a 300 mL Claisen flask fitted with a thermometer, a dropping funnel, and a condenser set for downward distillation, 40 mL of concentrated sulfuric acid and 100 mL of water were placed. The flask was heated to keep the internal temperature above 100 °C, and the diazonium solution was added through the dropping funnel. After the complete addition, the reaction was held under reflux for 50 min. The DMHB product was extracted with diethyl ether from the reaction medium, concentrated by an evaporator, and recovered by precipitation into hexane. DMHB obtained was further purified by GPC using tetrahydrofuran as an eluent. The yield was 698 mg (17%).

Synthesis of Polyether EDMB-10. Scheme 3 outlines the synthesis of liquid crystalline polyether EDMB-10. The phase-transfer-catalyzed polymerization was carried out for this preparation by using *o*-dichlorobenzene and an aqueous NaOH solution as reaction medium on the basis of the method previously reported.[7,8] 15 mL of a 3 N NaOH aqueous solution of 0.643 g (3.00 mmol) of DMHB and 15 mL of *o*-dichlorobenzene containing 0.900 g (3.00 mmol) of 1,10-dibromodecane were placed in a 100 mL reaction vessel. The mixture was heated to 93 °C under an argon atmosphere with vigorous stirring, and 0.102 g (0.300 mmol) of TBAH as a phase transfer catalyst was added quickly. After the 6 h reaction, the organic layer was separated at room temperature, washed with water and dilute HCl aqueous solution, and poured into methanol. The polymer thus recovered was purified by reprecipitation with *o*-dichlorobenzene/methanol. Finally, 0.939 g (85% yield) of the lightly yellow polymer was obtained as a powder.

Solid-State ^{13}C NMR Measurements. Solid-state ^{13}C NMR measurements were performed at various temperatures on a JEOL JNM-GSX200 spectrometer equipped with a variable temperature MAS system operating at 50.0 MHz under a static magnetic field of 4.7 T.[9−12] The detailed experimental conditions were described in our previous reports.[2,3] ^{13}C spin−lattice relaxation times (T_{1C}) were measured by using the CPT1 pulse sequence.[13] Solid-state ^{13}C NMR measurements at lower temperatures were conducted on a Chemagnetics CMX-400 spectrometer under a static magnetic field of 9.4 T. Almost the same experimental conditions were also used in this system. The sample for the NMR measurements was crystallized under an argon atmosphere by cooling from the melt at 140 °C through the liquid crystalline state at a rate of 1 °C/min.

Differential Scanning Calorimetry (DSC). A TA Instruments DSC2910 differential scanning calorimeter was used to measure the thermal transition behavior of EDMB-10.[2,3] All DSC runs were carried out for 2.2−10 mg samples under a nitrogen atmosphere at a rate of 10 °C/min.

Optical Microscopy. Thermal phase transitions and texture changes were observed with a Nikon OPTIPHOT2-POL optical polarizing microscope equipped with a Linkam LK-600PM hot stage. Powder-like EDMB-10 was placed on a glass slide and covered with a glass coverslip. Each sample was heated or cooled under a nitrogen atmosphere in the hot stage at a rate of 10 °C/min.

Results and Discussion

Structural Characterization. In the 400 MHz solution-state ^{1}H NMR spectrum measured at 60 °C for EDMB-10 in *o*-dichlorobenzene, resonance lines assigned to the OCH_2, $BrCH_2$, CH_3, OCH_2CH_2, and other CH_2 protons were found to clearly appear in the order of decreasing chemical shift value although most of the aromatic proton peaks were superposed upon the contributions from the solvent. The number-average molecular weight of EDMB-10, which was estimated from the ratio of the integrated intensities of the $BrCH_2$ and OCH_2 lines, is 8540.

Thermal Transition Behavior. The existence of the liquid crystalline phase for the EDMB-10 sample has been examined by DSC measurements and polarizing optical microscopic observations. DSC heating and cooling thermograms measured for EDMB-10 at a rate of 10 °C/min are shown in Figure 1. On the first cooling process from the melt (I), two exothermic peaks appear at about 113 and 98 °C. These two peaks were more clearly observed at faster cooling rates because the peak temperature of the lower-temperature side peak was significantly decreased with the increase of the cooling rate. In contrast, the two corresponding peaks were not well separately observed at any heating rate in the heating process, for example, as seen in Figure 1. Such

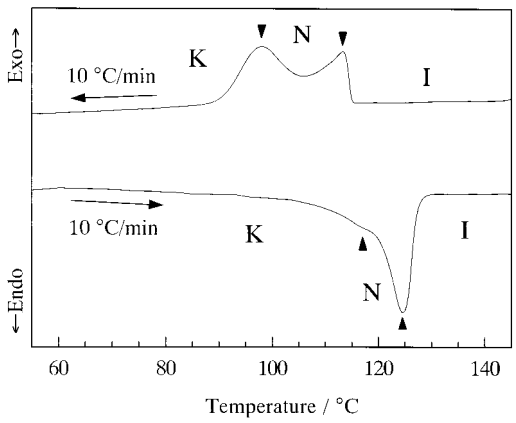

Figure 1. DSC thermogram of EDMB-10 recorded on cooling and subsequent heating at a rate of 10 °C/min.

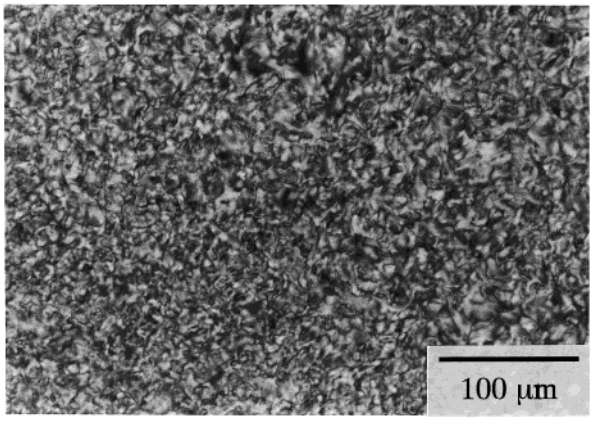

Figure 2. Polarizing optical microphotograph for EDMB-10 on cooling at a rate of 1 °C/min.

thermal transition behavior is completely different from the case of the liquid crystalline polyurethane (UDMB-10), where a single exothermic peak appears in the cooling process while two endothermic peaks are observed in the heating process.[2] The causes of the different thermal transitions of these liquid crystalline polymers will be discussed elsewhere by considering effects of hydrogen bonding after the completion of DSC measurements for the samples with different molecular weights at different cooling or heating rates. In the case of EDMB-10, polarizing optical observations have also confirmed, as shown in Figure 2, that the nematic liquid crystalline phase is really formed in the temperature region between the two DSC peaks in both cooling and heating processes. Moreover, it should be noted that a typical nematic schlieren texture was evidently observed by a polarizing light microscope when the EDMB-10 sample was quenched into ice−water from the melt at 160 °C.

CP/MAS and DD/MAS ^{13}C NMR Spectra at Different States. Figure 3 shows high-resolution solid-state ^{13}C NMR spectra measured at different temperatures for the EDMB-10 sample which was crystallized from the melt through the liquid crystalline phase at a cooling rate of 1 °C/min on the basis of the DSC measurements described above. The spectra of the solid state at 53.4 and 86.1 °C were obtained by CP/MAS ^{13}C NMR measurements, while the spectra in the liquid crystalline state (118.7 °C) and at the melt (151.3 °C) were measured by a $\pi/2$ single pulse sequence with a pulse repetition time of 5 s under dipolar decoupling (DD) and MAS. The assignment of each resonance line

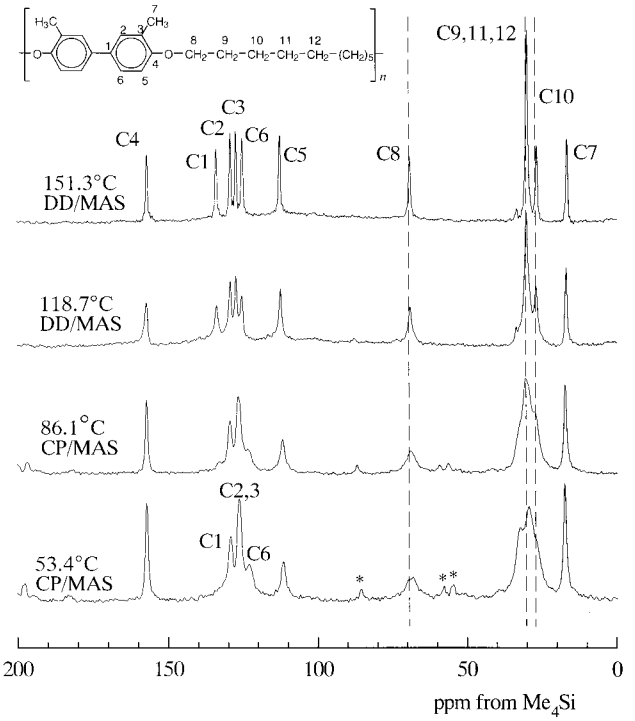

Figure 3. CP/MAS and DD/MAS ^{13}C NMR spectra of EDMB-10 measured at various temperatures. * indicates a spinning sideband.

was mainly made on the basis of the assignment established in solution by using the 2D ^{13}C INADEQUATE, C−H COSY, and H−H COSY spectra. In addition, the quaternary carbons of the phenylene group were discriminated in the CP/MAS spectra by the dipolar dephasing technique.

The chemical shifts of the respective CH_2 resonance lines at the melt and in the nematic liquid crystalline state have been found to be in good accordance with the values separately measured in solution, indicating that all C−C bonds of the CH_2 sequences undergo rapid *trans−gauche* exchanges in these two cases like in the solution state. On the other hand, some part of the C9, C11, and C12 resonance lines seems to shift downfield noticeably in the solid state at 53.4 °C compared with the single line for those carbons at the melt or in the liquid crystalline state, while the other CH_2 lines remain almost unchanged in their chemical shift values. These results suggest that some C−C bonds of the CH_2 sequence may adopt the *trans* conformation or the *trans*-rich *trans−gauche* exchange conformation. The detailed analysis of the conformation will be made later after the separation of the crystalline and noncrystalline contributions.

The resonance lines assigned to the phenylene carbons are also found to significantly change in positions in the CP/MAS spectra at 53.4 and 86.1 °C compared to those in DD/MAS spectra at higher temperatures; in particular, the C1 line shifts upfield by about 1.2 ppm. According to the crystal structure for liquid crystalline polyesters containing biphenylene groups as a mesogen, the respective phenylene rings are located in a position not significantly deviating from the coplanar position in the mesogen units.[14] Our preliminary wide-angle X-ray diffraction analysis[15] and molecular dynamics simulation[16] also suggested similar coplanar structure for the biphenylene group in the crystalline state for EDMB-10. Therefore, such coplanar structure may be

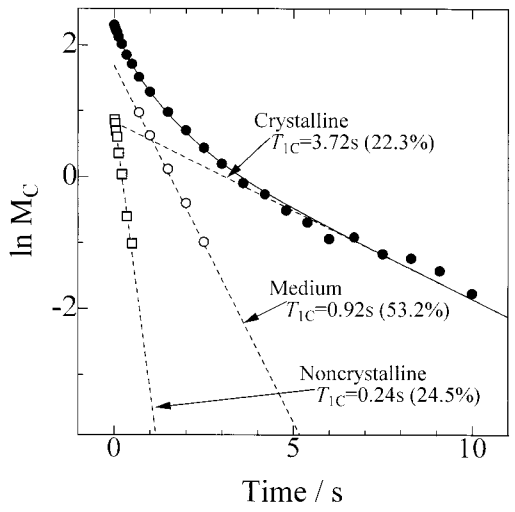

Figure 4. ^{13}C spin−lattice relaxation process of the C9, C11, and C12 resonance lines measured at 48 °C for EDMB-10 by the CPT1 pulse sequence.

destroyed by rapid rotation of each phenylene ring at least at the melt, resulting in the appreciable changes in chemical shifts.

^{13}C Spin−Lattice Relaxation Behavior. For the purpose of examining the crystalline−noncrystalline structure of EDMB-10, ^{13}C spin−lattice relaxation behavior has been measured at room temperature by the CPT1 pulse sequence.[9] In Figure 4 the logarithmic peak intensity of the C9−C12 resonance lines at 29.5 ppm obtained at 48 °C by the CPT1 pulse sequence is plotted against the decay time τ for the T_{1C} relaxation. The experimental points shown as filled circles appear not to be described by a single-exponential decay. Since this decay has been also found not to be described in terms of two exponentials, it has been resolved into three components having different T_{1C} values by the computer-aided nonlinear least-squares method as carried out for other liquid crystalline polymers previously reported.[2,3] The broken lines indicate exponential decays for the three components obtained by best fitting and the solid line is their composite curve. The experimental points are in good accord with the composite curve, indicating the existence of three components with different molecular mobilities for the C9−C12 lines at reasonably high reliability.

Since longer T_{1C} values imply less molecular mobility under the present experimental condition, the longest T_{1C} component should be assigned to the crystalline component as done for liquid crystalline polyurethane.[2] Wide-angle X-ray diffraction patterns and DSC thermograms also support the presence of the crystalline component in this sample. The other two components may be assigned to the medium and noncrystalline components in the order of decreasing T_{1C} value. Here, the noncrystalline component should correspond to the supercooled liquid crystalline component, because the sample was crystallized from the melt through the nematic liquid crystalline phase. The content of the medium component is not clear at present, but it may be located in the interfacial region between the crystalline and noncrystalline regions.

In Table 1 is summarized the T_{1C} values for the representative carbons forming the spacer CH_2 sequences and the mesogen units for EDMB-10 obtained at 48 °C by an analysis similar to that as shown in Figure 4. For comparison, the corresponding T_{1C} values are also presented for the UDMB-10 sample previously reported.[2] Interestingly, only two components are recognized for the mesogen carbons for each sample, whereas there exist three components for the spacer carbons that correspond to the crystalline, medium, and noncrystalline components. This fact suggests that the low molecular mobility of the rigid mesogen units may hinder the discrimination among morphologically different components based on T_{1C} differences. For example, the mesogen units located in the interfacial region close to the crystalline region will not be appreciably different in molecular mobility from those in the crystalline region. Similarly, the molecular mobility of the mesogen groups in the noncrystalline region may not be significantly enhanced compared to that in the interfacial region closely connecting to the noncrystalline region. It should be noted here that T_{1C} values of the crystalline components of the spacer CH_2 carbons for EDMB-10 are as short as about 4 s compared to the values of 190−230 s for the UDMB-10 sample. This result suggests that the spacer CH_2 sequences undergo much enhanced molecular motion even in the crystalline region. A characteristic spacer conformation allowing such high molecular mobility will be clarified by the evaluation of the ^{13}C chemical shifts of the spacer CH_2 carbons as described later. The shorter T_{1C} values of the mesogen carbons in the crystalline component for EDMB-10 may be also associated with higher molecular mobility of the mesogen units probably coupled with the enhanced mobility of the spacer CH_2 sequences.

^{13}C NMR Spectra of the Three Components. Figure 5 shows ^{13}C NMR spectra of the crystalline, medium, and noncrystalline components for the C9−C12 resonance lines, which were separately recorded by using the difference in T_{1C} as follows: The spectrum of the crystalline component was selectively measured as the longest T_{1C} component by the CPT1 pulse sequence[9] with a T_{1C} decay time τ of 5 s. The spectrum of the medium component was obtained by subtracting the spectrum of the crystalline component from the spectrum measured by the CPT1 pulse sequence with $\tau = 2$ s, which is sufficiently long for the noncrystalline component to completely disappear. As for the noncrystalline component, the spectrum was measured by the $\pi/2$ single pulse sequence by setting the pulse repetition time to 0.1 s, although some minor contributions from other components may be included in this spectrum.

The chemical shift of each resonance line is almost the same for the crystalline and medium components as clearly seen in Figure 5, indicating that both components have the same conformation for the methylene sequence associated with these CH_2 carbons. In contrast, the C9−C12 resonance lines for the noncrystalline component significantly shift upfield compared to the corresponding lines for the crystalline and medium components. To examine the conformation of the CH_2 sequence for each component by analyzing the chemical shifts of the respective lines considering the *γ-gauche* effect,[17] line shape analyses have been carried out for the crystalline and noncrystalline components.

Figure 6 shows the result of the line shape analysis for the crystalline component. Here, each line is assumed to be described by a Lorentzian curve. It is found that the resonance lines located at about 32−33 ppm are well resolved into three Lorentzian curves, which correspond to the resonance lines for C9, C11, and C12 carbons. These three lines should be introduced by

Table 1. ^{13}C Spin−Lattice Relaxation Times of the Spacer and Mesogen Carbons in the Respective Components Measured at 48 °C for EDMB-10 and UDMB-10

	T_{1C}/s					
	spacer			mesogen		
component	CH_2[a]		OCH_2	q C[b]	CH[c]	CH_3
EDMB-10						
crystalline	3.72	4.36	5.16			
medium	0.92	1.06	0.94	30.2	12.3	13.8
noncrystalline	0.24	0.23	0.39	7.5	3.0	3.8
UDMB-10[d]						
crystalline	227	191	217			
medium	22.6	13.3	18.8	212	187	65.3
noncrystalline	1.0	0.48	0.95	19.0	10.8	6.5

[a] At 32 and 29 ppm for EDMB-10; at 32 and 27 ppm for UDMB-10. [b] Quaternary carbons; at 157 ppm for EDMB-10; at 133 ppm for UDMB-10. [c] At 111 ppm for EDMB-10; at 125 ppm for UDMB-10. [d] Reference 2.

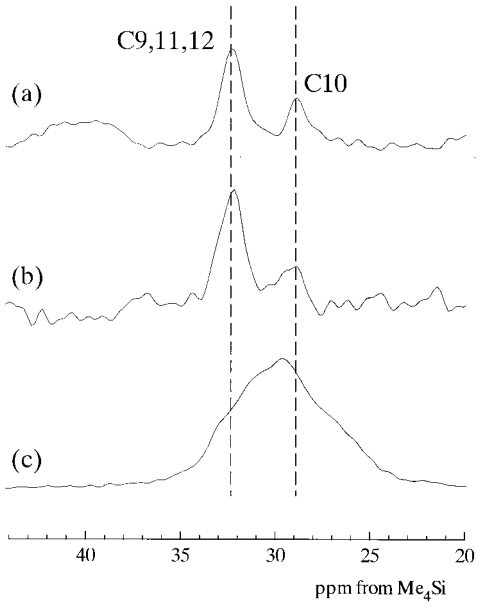

Figure 5. ^{13}C NMR spectra of different components separately recorded at 48 °C for EDMB-10: (a) crystalline, (b) medium, and (c) noncrystalline.

considering that similar three lines with almost the same chemical shifts are necessary for best fit for the medium component produced in addition to the noncrystalline component as shown later. Moreover, the resonance line located at about 28.8 ppm is well described by one Lorentzian corresponding to the C10 carbon.

In contrast, the C9−C12 resonance lines for the noncrystalline component are resolved into more different constituent lines as seen in Figure 7. This spectrum may contain minor contributions from the medium component, because the T_{1C} values for the component are not sufficiently long compared to the pulse repetition time (0.1 s) employed in this case. Therefore, these contributions are introduced as four small Lorentzians for the C9−C12 carbons in addition to four somewhat stronger Lorentzians assigned to the C9−C12 carbons for the noncrystalline component. Here, the chemical shift values of the four former Lorentzians should agree with those of the corresponding Lorentzians for the crystalline component shown in Figure 6 because the respective chemical shifts of the CH_2 carbons coincide with each other for the crystalline and medium components as shown in Figure 5. Moreover, the different intensities of the C9−C12 lines obtained by this line shape analysis may be possibly due

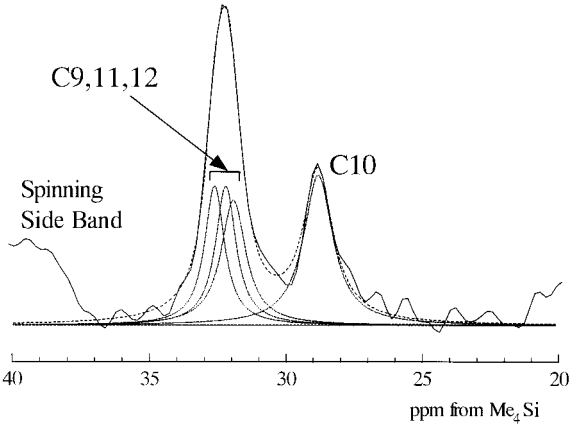

Figure 6. Line shape analysis for the CH_2 resonance lines of the crystalline component for EDMB-10.

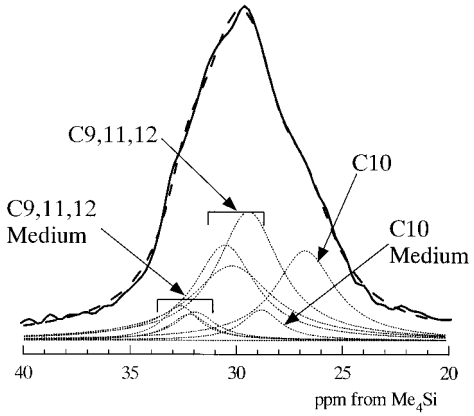

Figure 7. Line shape analysis for the CH_2 resonance lines of the noncrystalline component for EDMB-10.

to the difference in T_{1C} for these carbons. As a result of such a line shape analysis, a composite curve, denoted by a broken line, for the eight Lorentzians is in good accord with the observed spectrum indicated by a thick solid line. According to this analytical result, the C9−C12 chemical shifts of the noncrystalline component are found to evidently shift upfield compared to the corresponding values for the medium or crystalline component. However, these chemical shift values including the value for the C8 carbons coincide well with the corresponding values obtained for the EDMB-10 sample in the nematic liquid crystalline state or at the melt. This fact clearly indicates that all C−C bonds of the spacer CH_2 sequence for the noncrystalline component should also undergo rapid exchanges between the *trans* (*t*) and *gauche* (*g*) conformations, which is denoted by *x*, like in

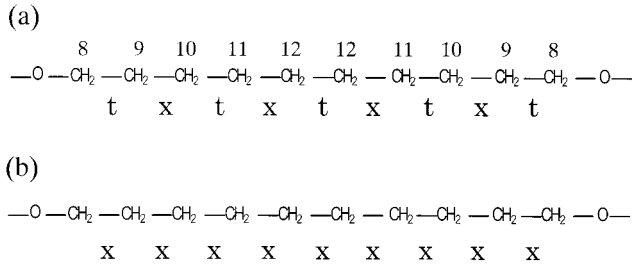

Figure 8. Chain conformations for the spacer CH_2 sequences in different components in EDMB-10: (a) crystalline and medium components; (b) noncrystalline component. *t* and *x* indicate *trans* and *trans*−*gauche* exchange conformations, respectively.

the liquid crystalline and isotropic phases as schematically shown in Figure 8b.

Next, we examine the conformation of the CH_2 sequence for the crystalline component by comparing the ^{13}C chemical shifts with those for the noncrystalline component. Since the chemical shift for the C8 carbons of the crystalline component agrees well with the value for the noncrystalline component as shown in Figure 3, the C9−C10 bonds should be subjected to the rapid *t*−*g* exchange conformation (*x*). In contrast, the other CH_2 resonance lines for the crystalline or medium component are found to undergo about 2.5 ppm downfield shifts compared to the corresponding lines for the noncrystalline component as shown in Figure 7. This fact may indicate that each CH_2 line for the crystalline component undergoes only a half of the normal *γ-gauche* effect.[17] On the basis of these results, the conformation of the CH_2 sequence will be reasonably proposed for the crystalline component as shown in Figure 8a: First, such a decrease in the *γ-gauche* effect for the C11 carbons suggests that the C12−C12 bond will be *t* because the C9−C10 bond is *x* as described above. Moreover, the C10−C11 bond may be determined as *t* by considering the *γ-gauche* effect for the C9 carbons, if the O−C8 bond is assumed to adopt the same conformation as that at the melt or in the liquid crystalline state as discussed later. A similar evaluation for the C12 and C10 carbons in this order also leads to the conclusion that the C12−C11 and C8−C9 bonds are *x* and *t*, respectively.

As for the O−C8 bond for the crystalline component, the same conformation as that at the melt or in the liquid crystalline sate has been assumed as described above. The reason for such an assumption is based on the result that an extraordinary conformation must be introduced for the crystalline component without this assumption. Namely, if a conformational change inducing about 2.5 ppm downfield shift for the C9 line occurs for the O−C8 bond in the crystalline component, the C10−C11 bond must adopt the *x* conformation like in the noncrystalline component. As a result of further evaluation of the C12 and C10 resonance lines, it is suggested that the spacer CH_2 conformation may be described as *xxxtttxxx* in this case instead of *txtxtxtxt* as shown in Figure 8. Since the successive *xxx* conformation should be energetically prohibited especially in the crystalline region, the assumption made above must be plausible.

Our recent molecular dynamics simulation also supports the existence of the *txtxtxtxt* conformation for the spacer CH_2 sequence in the crystalline region.[16] In this simulation Cerius[2] (Version 4.2 MatSci., Molecular Simulations Inc.) was employed with the PCFF force field. As a crystal model, 16 chains composed of five mesogen units and three spacer CH_2 sequences were set in an appropriate cell under periodic boundary conditions. The initial structure was obtained by the energy minimization at 100 K, and the cell parameters obtained were well close to the unit cell parameters estimated by the WAXS analysis for the uniaxially oriented EDMB-10 sample separately prepared. Above about 300 K, single *gauche* conformations were found to be sometimes introduced in the C9−C10 bonds in close relation to the change in torsion angle from 90° to 180° (*t*) for the O−C8 bonds. Such a cooperative change in torsion angle seems inevitable to keep almost constant the distance between the mesogen units along the molecular chain in the crystalline phase in the case of single *gauche* introduction. Moreover, coupled two-*gauche* introduction was found to occur at higher temperatures above about 400 K along the spacer CH_2 sequences. Since the positions of the *gauche* conformation were two of the C9−C10, C11−C12, C12−C11, and C10−C9 bonds at nearly equal probabilities, the time-averaged conformation was determined to be *txtxtxtxt*, in good accord with the experimental result shown in Figure 8. Wide-angle X-ray diffraction analysis of the crystal structure for another type of liquid crystalline polyether also suggested that the spacer CH_2 sequences seemed "melted" in the crystalline region.[18] However, the CH_2 sequences may not be completely conformationally random, but they must adopt some particular conformation composed of the *t* and *x* conformations. More detailed discussion will be made elsewhere, including the molecular motion and orientation of the mesogen groups after the completion of the MD simulations.

CP/MAS ^{13}C NMR Measurements at Lower Temperatures. To obtain further information on the spacer conformation, CP/MAS ^{13}C NMR measurements were performed at lower temperatures below room temperature. Figure 9 shows the CP/MAS ^{13}C NMR spectra of EDMB-10 at lower temperatures, which contain the contributions from the three components. The contribution at about 29.5 ppm, which is ascribed to the C9, C11, and C12 carbons for the noncrystalline component, seems to significantly shift downfield with decreasing temperature. This fact suggests that the *t*−*g* exchange conformation for the C10−C11 and C12−C12 bonds becomes somewhat *trans* rich at lower temperatures. In contrast, no downfield shift is observed for the contribution at about 32.5 ppm that is mainly assigned to the C9, C11, and C12 carbons in the crystalline and medium components. This fact indicates that the *t*−*g* exchanges are still active on a time scale higher than 100 s^{-1} even at −150 °C in the crystalline region without fixation to the *trans* or *gauche* conformation.

Conclusions

A new type of liquid crystalline polyether (EDMB-10), which has the same mesogen and spacer units as those for liquid crystalline polyurethane (UDMB-10) previously reported, has been polymerized from 3,3′-dimethyl-4,4′-hydroxybiphenyl and 1,10-dibromodecane. The structure and chain conformation of the spacer CH_2 sequence have been characterized mainly around room temperature for the sample crystallized from the melt through the nematic liquid crystalline phase by solid-state ^{13}C NMR spectroscopy and the following conclusions have been obtained.

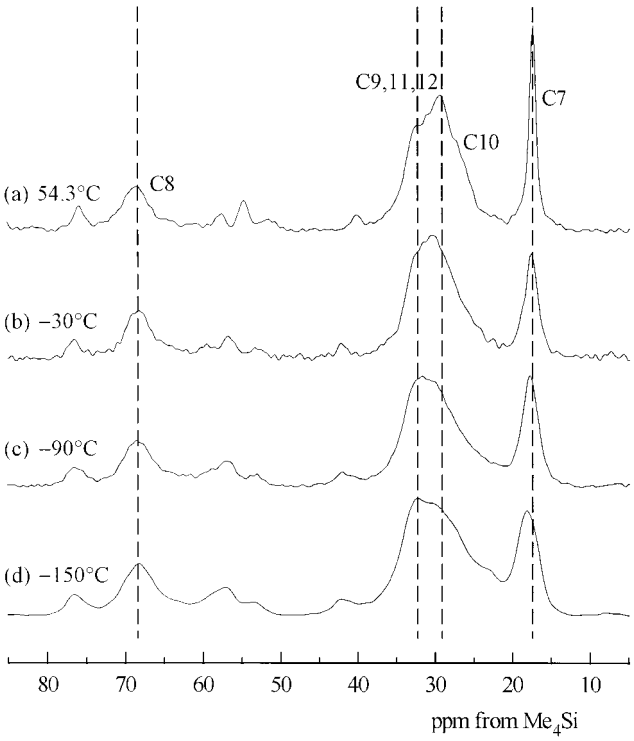

Figure 9. CP/MAS ^{13}C NMR spectra measured for EDMB-10 at various temperatures lower than room temperature.

(1) ^{13}C spin−lattice relaxation time (T_{1C}) analyses have revealed the existence of three components with different T_{1C} values for the spacer CH_2 sequences around room temperature. These components are assigned to the crystalline, medium, and noncrystalline components in the order of decreasing T_{1C}. The T_{1C} values of the spacer CH_2 and mesogen carbons of the crystalline component are remarkably shorter for EDMB-10 compared to those for UDMB-10, suggesting much enhanced molecular motion in the crystalline region for the EDMB-10 sample.

(2) The spectra of the respective components have been separately recorded by using the difference in T_{1C}, and the conformation of the CH_2 sequences has been clarified by the evaluation of ^{13}C chemical shifts in terms of the *γ-gauche* effect: For the crystalline and medium components, the CH_2 sequences are found to adopt the alternate *trans* (*t*) and *trans−gauche* exchange (*x*) conformation (*txtxtxtxt*), in good accord with much enhanced molecular motion for the CH_2 sequences as suggested by very short T_{1C} values. Our separately performed molecular dynamics simulation also supports the existence of such an interesting chain conformation in the crystalline region for EDMB-10.

(3) In the noncrystalline component, which corresponds to the supercooled liquid crystalline component, all the C−C bonds of the CH_2 sequences are found to be in the rapid *trans−gauche* exchange conformation (*xxxxxxxxx*), reflecting the same conformation in the nematic liquid crystalline state or at the melt. This conformation is greatly different from the *ttxtxtxtt* conformation for the noncrystalline component in the UDMB-10 sample, suggesting some role of intermolecular hydrogen bonding to induce the latter conformation in the liquid crystalline phase.

Acknowledgment. This work was supported by Grant-in-Aid for Scientific Research (No. 12450384) from the Ministry of Education, Culture, Sports, Science and Technology, Japan.

References and Notes

(1) For example: (a) Collyer, A. A., Ed.; *Liquid Crystal Polymers: From Structure to Applications*; Polymer Liquid Crystals Series 1; Chapman & Hall: London, 1992. (b) Carfagna, C., Ed.; *Liquid Crystalline Polymers*; Pergamon: Oxford, U.K., 1994. (c) Acierno, D., Collyer, A. A., Eds.; *Rheology and Processing of Liquid Crystalline Polymers*; Polymer Liquid Crystal Series 2; Chapman & Hall: London, 1996. (d) Collings, P. J., Patel, J. S., Eds.; *Handbook of Liquid Crystal Research*; Oxford University Press: New York, 1997.
(2) Ishida, H.; Kaji, H.; Horii, F. *Macromolecules* **1997**, *30*, 5799.
(3) Ishida, H.; Horii, F. *Polymer* **1999**, *40*, 3781.
(4) *Org. Synth. Collect. Vol. I*, p 404.
(5) *Org. Synth. Collect. Vol. II*, p 145.
(6) *Org. Synth. Collect. Vol. III*, p 130.
(7) Shaffer, T. D.; Percec, V. *J. Polym. Sci., Polym. Lett. Ed.* **1985**, *23*, 185.
(8) Shaffer, T. D.; Jamaludin, M.; Percec, V. *J. Polym. Sci., Polym. Chem. Ed.* **1986**, *24*, 15.
(9) Masuda, K.; Kaji, H.; Horii, F. *Polym. J.* **2001**, *33*, 356.
(10) Ohira, Y.; Horii, F.; Nakaoki, T. *Macromolecules* **2000**, *33*, 5566.
(11) Kuwabara, K.; Kaji, H.; Horii, F. *Macromolecules* **2000**, *33*, 4453.
(12) Ohira, Y.; Horii, F.; Nakaoki, T. *Macromolecules* **2000**, *33*, 1801.
(13) Torchia, D. A. *J. Magn. Reson.* **1981**, *44*, 117.
(14) Li, X.; Brisse, F. *Macromolecules* **1994**, *27*, 7718.
(15) Doho, T.; Nozaki, K.; Yamamoto, T.; Murakami, M.; Ishida, H.; Horii, F. *Polym. Prepr., Jpn.* **2001**, *50*, 586; to be published.
(16) Ishida, H.; Maekawa, Y.; Horii, F.; Yamamoto, T. *Polym. Prepr., Jpn.* **2001**, *50*, 517; to be published.
(17) Tonelli, A. E. *NMR Spectroscopy and Polymer Microstructure: The Conformational Connection*; VCH Publishers: New York, 1989.
(18) Unger, G.; Feijoo, J. L.; Percec, V.; Yourd, R. *Macromolecules* **1991**, *24*, 953.

MA011113L